Apparent failure and cryptic success of disease control via intermediate host population reduction: Density dependence in copepods has implications for Guinea worm disease transmission

Authors: **Nadia Raytselis[1]**, Maya Risin[1], Layla Steinbock[1], Logan T. Story[1], Jane Miller[1], Ta'Nyia Heard[1], Kevin Xie[1], Ella Rintala[1], Inesha Gupta[1], Stephanie Gutierrez[1], Alexander Strauss[2,3,4], David J. Civitello[1]

1. Department of Biology, Emory University, Atlanta, GA, 30322, USA
2. Odum School of Ecology, University of Georgia, Athens, GA, 30602, USA
3. Center for the Ecology of Infectious Diseases, University of Georgia, Athens, GA, 30602
4. River Basin Center, University of Georgia, Athens, GA, 30602

Abstract

Pest control often causes high mortality, reducing population density but enabling recovery when survivors are freed from intraspecific competition and density dependent demographic rates. Understanding these demographic responses is critical for effective management, especially when life stages differ in the harm they cause. We evaluated mortality-based management of intermediate copepod hosts to control Guinea worm (GW) transmission, combining mathematical models with a population dynamics experiment designed to mimic current pesticide control methods across a range of intensities. Despite initial reductions in density, copepods recovered so rapidly that control appeared to fail, enabled by extremely fast maturation rates in low-density populations. However, model simulations of GW transmission showed that although total and stage-specific densities rebounded, infectious adult copepods —the proximate cause of infections—were strongly suppressed, indicating cryptic success. Ultimately, this study highlights the importance of understanding mechanisms of density dependence when designing and optimizing pest control interventions.

Introduction

Elucidating the mechanisms that regulate populations is a fundamental goal of population ecology. Negative feedbacks on population growth emerge because of competition for space (Sebens 1982) and resources (Svanbäck & Bolnick 2007), degradation of the environment (Calizza *et al.* 2017), or other mechanisms that reduce individual performance as density rises (Lu & Wang 2025; Stockseth *et al.* 2025). Reductions in birth rates (Gotelli 2008) and increases in death rates are ubiquitous inhibitors of population growth (Hixon & Jones 2005). In populations with stage structure, negative density dependence can also arise through maturation rates or cannibalism (Park *et al.* 1965; Dennis *et al.* 2001; Walker *et al.* 2021). Despite the reality that all populations experience negative density dependence (lest they increase infinitely), it remains challenging to identify which form(s) operate most strongly for any species and few studies attempt to do so (Kaspersson *et al.* 2013).

The forms of density dependence are particularly relevant for pest control, because interventions are designed to reduce pest density. This reduction is often followed by rapid recovery, driven by relaxed density dependence (Karatayev *et al.* 2015) or potential acquisition of resistance (Cao *et al.* 2025), limiting benefits and necessitating repeated interventions (McIntire & Juliano 2018). The ensuing dynamics of repeated pest suppression and recovery can be highly sensitive to density-dependent vital rates (Smith 1997). For example, strong negative density dependence can cause compensation or overcompensation, the phenomena in which control efforts actually increase the density or biomass of some or all life stages (Karatayev *et al.* 2015; de Roos 2020; Grosholz *et al.* 2021). Even when interventions successfully reduce density, populations can rebound faster than expected if the remaining individuals are released from density-dependent reductions in maturation or birth rates (Karatayev *et al.* 2015). Such responses

may be strongest in stage-structured populations, where removal of more competitive classes, or reductions in density overall, elicit stage-specific compensatory responses (Karatayev *et al.* 2015). Thus, delineating the form(s) and magnitude of density dependence can improve management of the ecological issues that pests cause, such as disease transmission, crop losses, and biodiversity harm.

Here we combine an experiment manipulating pest control intensity with mechanistic modeling to identify which density-regulating mechanisms affect copepods, the intermediate hosts of the Guinea worm (GW) parasite, *Dracunculus medinensis*. Copepods exhibit stage-structured populations (van den Bosch & Gabriel 1994) and experience repeated control interventions due to their role in GW transmission (Gindola *et al.* 2022). Guinea worm disease (GWD) is a globally impactful infectious disease, causing disability and negative economic impacts in endemic areas (Pellegrino *et al.* 2022). Cyclopoid copepods are obligate intermediate hosts that become infected through consumption of GW larvae and facilitate transmission to humans and other definitive mammalian hosts (Simonetti *et al.* 2023). GWD has been targeted for eradication for several decades (World Health Organization 1986), with few cases remaining across five endemic countries (World Health Organization 2025). In GW-endemic regions, application of the pesticide Abate™ (active compound: temephos) is a major component of eradication efforts (Gindola *et al.* 2022). Abate™ can cause >99% immobilization of copepods in laboratory studies (Grunert *et al.* 2022), although copepod species vary widely in their sensitivity (Hanazato *et al.* 1989; Leboulanger *et al.* 2011). In Abate™-treated sites, copepod populations often exhibit immediate reductions in density, but routinely recover, necessitating application at 28-day intervals to support eradication (Gindola *et al.* 2022). The density-

89 dependent demographic responses of these intermediate hosts – along with implications for
90 disease control – are unknown.

91 Copepod stage structure has implications for both their population dynamics and GW
92 transmission. Neonatal copepods (nauplii) are too small to consume GW larvae, but larger
93 juveniles (copepodites) and adults can consume parasites and become infected (McCullough
94 1983; Bimi 2007). Once ingested, parasites molt twice over 10-16 days within the copepod
95 before maturing into third stage larvae, the only stage infectious to definitive hosts that imbibe
96 infected copepods (Gonzalez Engelhard *et al.* 2021). Additionally, adults can cannibalize nauplii
97 (van den Bosch & Santer 1993). Finally, public health officials have shared anecdotally that
98 adults and copepodites may be more sensitive to Abate™ than nauplii. Critically, the
99 consequences of these stage-structured interactions for disease management are unknown.

100 To understand copepod demographic responses to episodic culling, and to predict
101 implications for disease control, we conducted a mesocosm experiment that mimicked the 28-
102 day treatment interval of Abate™ by physically removing copepods (either applied equally
103 across stages or biased toward larger individuals). We hypothesized that more intense
104 interventions (higher removal percentages) would cause greater reductions in population density,
105 but that relaxed density dependence might cause compensation or overcompensation between
106 interventions. Further, we speculated that these effects would be more pronounced in populations
107 where both size classes were removed. Finally, we hypothesized that even if copepods
108 rebounded rapidly ('apparent failure'), risk of parasite transmission might remain low ('cryptic
109 success') due to high adult turnover rate and the two-week period required for parasite
110 development from first stage to infectious third stage larvae.

111 Surprisingly, all interventions failed to reduce mean copepod density over the 14-week
112 intervention period. Copepods recovered extremely rapidly due to relaxed density dependence on
113 maturation rates. However, despite this apparent failure, model simulations indicate that
114 interventions may still reduce transmission risk by specifically suppressing the density of
115 infectious copepods. These results illustrate how density-dependent mechanisms interact with
116 transmission biology to drive cryptic success of control. Stage structure is a key feature of the
117 biology of many pest species, e.g., root-feeding crop pests (Johnson & Rasmann 2015) and
118 mosquito vectors of human diseases (Neale & Juliano 2019; Walker *et al.* 2021), and control
119 interventions often focus on specific life stages that are not always the proximate cause of harm,
120 e.g., larvicides to control pathogens transmitted by adult mosquitoes (Choi *et al.* 2019). Thus,
121 understanding the underlying mechanisms of stage-structured density dependence could enhance
122 our ability to address a diverse range of ecological challenges.

123 **Methods**

124 ***Copepod Maintenance and Propagation***

125 We obtained *Eucyclops sp.* copepods isolated near Mandelia, Chad, an active focus of GW
126 transmission. We maintained copepods in 0.5x HHCOMBO artificial lake with 1X
127 micronutrients (hereafter COMBO; Kilham *et al.* 1998) in 1 L beakers at 26C with a 12:12
128 daylight cycle. We fed them 7.5 mg/L of powdered egg yolk (Judee's, Plain City, Ohio)
129 suspension every Monday, Wednesday, and Friday (M/W/F), and transferred copepods to new
130 media approximately every three weeks by sieving. Once densities reached ~500-1,000
131 copepods/L, we poured one 1 L culture into 42, 15 L propagation tanks with 4 L COMBO.

132 ***Mesocosm Setup, Sampling, and Experimental Design***

133 On September 20th, 2024, we filled 60 15 L tanks with 5 L COMBO and added 1.5 mg/L
134 powdered egg yolk on Monday/Wednesday/Friday to establish microbial communities. On
135 October 2nd, 2024 (day 0), we introduced copepods to tanks by adding seven 1 L aliquots
136 collected randomly from the 42 propagation tanks after stirring to homogenize. We then added
137 COMBO to 15 L total and fed tanks 7.5 mg/L every Monday/Wednesday/Friday throughout the
138 experiment. We replaced water weekly to counteract evaporation (<1 L/tank/week).
139 We maintained the experiment for 126 days and sampled every Friday starting on day 2.
140 To sample, we homogenized tanks (stirring with a plastic paddle) and collected a 500 mL surface
141 grab sample with a beaker. We replaced this volume with COMBO. We intervened at 28-day
142 intervals (days 8, 36, and 64) to mimic the field use of Abate™ (Gindola *et al.* 2022). We
143 implemented mechanical removal, rather than Abate™, to enable consistent gradients of size-
144 biased and size-unbiased removal. We factorially crossed intervention type (equal vs. size-
145 biased) with the percent of the volume (i.e., copepod population) removed (0-90%: 0, 10, 20, 30,
146 40, 50, 60, 70, 80, or 90%). For size-biased removal, we sieved water through 100 µm nylon
147 screen, capturing adults, juveniles, and larger nauplii, and returned the water and smaller nauplii
148 to tanks. For size-unbiased (i.e., equal) removal, we replaced the volume removed with fresh
149 COMBO. In Supplemental S7, we provide methodological details and results on the accuracy of
150 interventions relative to nominal treatment levels. After the first intervention, we converted the
151 10% and 20% treatments to 95% and 98% for the following interventions, because low initial
152 intensities caused negligible effects, and higher removal rates better match the stated efficacy of
153 the Abate™ (Grunert *et al.* 2022). On weeks with interventions, we sampled on Thursday and
154 intervened on Friday. We "skipped" the intervention scheduled for day 92 to observe responses
155 to treatment lapse, as can occur in the field due to inaccessibility from flooding.

156 ***Copepod Counting***

157 We quantified copepods by sieving the 500 mL samples with 35 µm mesh (which captures all
158 stages) and preserving them in 10 mL ethanol. We gently resuspended the samples and examined
159 successive 1 mL aliquots at 10-25x magnification on a dissecting microscope until counting ≥ 50
160 copepods or screening the entire sample. We counted copepods in three morphologically
161 discernible categories (nauplii, juveniles and eggless adults, and adult females with eggs).

162 ***Statistical Analysis of Intervention Effects on Copepod Density***

163 We conducted all analyses in the R Computing Language v4.3.2 (R Core Team 2023). We tested
164 for differences in mean population density over the first 14 weeks, when treatments were applied
165 "on schedule", using planned contrasts between all interventions versus controls (Dunnett's tests;
166 package emmeans (Lenth 2025). This analysis used a Generalized Linear Model (package
167 glmmTMB; Bolker 2017) with mean density as the response, removal proportion, removal type,
168 and their interaction as predictors, and the Gamma error distribution with a log link function.

169 ***State Space Modeling (SSM) of Copepod Population Dynamics***

170

171 We built a stochastic population dynamic model and simultaneously fit it to all time series of
172 observations from the experiment using the Partially Observed Markov Process (POMP)
173 framework and the panelPomp package (Carles Bretó 2025). We connected likelihood estimates
174 generated by the function pfilter() to an adaptive Markov Chain Monte Carlo (MCMC) sampler
175 in the adaptMCMC package to conduct Bayesian inference, with priors informed by auxiliary
176 experiments (Supplemental S2). POMP models are ideal for population dynamics data
177 (Newman *et al.* 2023) where state variables (the "true" abundances of nauplii, juveniles, and
178 adults) are partially observed as empirical subsample counts of nauplii (N_{obs}), juveniles/adult

males/adult females with no eggs (JOA_{obs} = "juveniles and other adults"), and adult females (AF_{obs}) (Carles Bretó 2025).

We implemented the model by specifying ordinary differential equations that describe deterministic rates of change in the densities of nauplii, *N*, juveniles, *J*, and adults, *A*. In this model (Equations 1-6), nauplii are born, develop into juveniles, die from background causes, and are cannibalized by adults. Juveniles mature from nauplii, develop into adults, and die of background causes. Adults mature from juveniles, birth and cannibalize nauplii, and die of background causes. Critically, birth rate (*b)*, stage-specific death rates (d_i, with $i = N, J, or\ A$), and stage-specific maturation rates (m_i, with $i = N\ or\ J$) depend exponentially on density, with each stage potentially contributing differentially to density dependence via their impact on the competitive environment (i.e., c_J and c_N represent the competitive effects of juveniles and nauplii relative to adults). We allowed adults to cannibalize nauplii following a linear functional response with attack rate α. On intervention days, we incorporated removal as additional mortality on relevant stage(s). During all interventions, we assumed juveniles and adults were removed according to treatment. We assumed nauplii were removed proportionally in size-unbiased removal treatments and used a prior informed by an auxiliary experiment that showed size-biased sieving removed approximately 45% of nauplii (Supplemental S5).

$$\frac{dN}{\mathrm{dt}} = b(N,J,A)\frac{A}{2} - m_N(N,J,A)N - d_N(N,J,A)N - \alpha NA \qquad \text{Eq. 1}$$

$$\frac{dJ}{dt} = m_N(N,J,A)N - m_J(N,J,A)J - d_J(N,J,A)J \qquad \text{Eq. 2}$$

$$\frac{dA}{dt} = m_J(N,J,A)J - d_A(N,J,A)A \qquad \text{Eq. 3}$$

with density-dependent functions:

$$b(N,J,A) \ = \ b_M e^{\left(-\frac{c_b}{V}(c_N N + c_J J + A)\right)} \qquad \text{Eq. 4}$$

$$m_i(N,J,A) = m_{i0}e^{\left(\frac{-c_m}{V}(C_N N + C_J J + A)\right)} \quad \text{Eq. 5}$$

$$d_i(N,J,A) = d_{i0}e^{\left(\frac{c_d}{V}(C_N N + C_J J + A)\right)} \quad \text{Eq. 6}$$

To simulate the dynamics of the latent (or "true and unobserved") state of the system we assumed demographic stochasticity and implemented the model with a one-day time step. Specifically, we tracked individuals transitioning through stages or dying using random multinomial draws where the probability of three potential outcomes for any individual (remaining in the same state, maturing to the next state, or dying) depends on the relative rates of each process. We assumed births followed Poisson random draws depending on the total birth rate. Our observations differentiate N_{obs}, AF_{obs}, and JOA_{obs}. We assumed that each observation followed a negative binomial distribution with a common overdispersion parameter. For each observation, we assumed the predicted count was determined by the product of the abundance of individuals of that stage at time t, the proportion of the tank sampled (always 0.5/15 L = 3.3%), and the proportion of the 10 mL subsample counted. To align true and observed categories, we assumed a 50:50 sex ratio with female reproduction, with adult females releasing eggs every third day and appearing eggless for one day in each three-day interval (personal observation TDH). With this model specified, we used the pfilter() function in panelPomp to estimate model likelihoods from the data. To maintain variance in log-likelihoods < 1 (Endo *et al.* 2019), we used 20 particles per likelihood estimation, resulting in variances of approximately 0.5. We ran 32 MCMC chains, with dispersed initial parameter sets for 250,000 iterations each, permitting adaptation during the first 50,000 iterations (burn-in), which we later discarded.

Model-derived estimates of density dependence

223 We used model-derived functions of density dependence, observed densities, and stage structure
224 from the experiment to visualize how the competitive environment shaped demographic rates.
225 We thinned chains to every 1,000th iteration, and calculated per-capita birth, death, cannibalism,
226 and maturation rates across a density gradient from 0 to 6,000 individuals/L for each parameter
227 set (the density range observed in the experiment). We fixed stage structure along this density
228 gradient (5.5% adults, 39% juveniles, and 55.5% nauplii, 1:7:10 ratio), based on the average
229 proportions in the experiment. We then generated the mean and 95% CI interval of posterior
230 predictions for each demographic rate along the gradient.

231 ***Compartmental (ODE) stage structured model with interventions and infection***

232 Large-scale experiments with viable GW larvae are currently infeasible. Therefore, we extended
233 our model to gain applied insights into disease control. The extended model (Eq. S1-S11 in
234 Supplemental S1) allows parasites to infect adult copepods. We implemented a distributed
235 developmental delay (Hurtado & Kirosingh 2019) for copepods transitioning from exposed to
236 infectious to definitive hosts (Supplemental S1). This approach uses the "linear chain trick"
237 (Hurtado & Kirosingh 2019) to implement a variable time lag, as we hypothesized this delay
238 could be important for differentiating successful population regulation from successful disease
239 control. Once an adult copepod consumes the parasite, it takes approximately 15 days to become
240 infectious (Lindquist & Cross 2017). Thus, we added a developmental delay of approximately 15
241 days by implementing a chain of 60 exposed stages that copepods transition through at a rate of
242 4.3 d^{-1}, yielding a 15.45 ± 1.82-day delay from exposure to infectiousness.

243 Estimates of the force of infection for copepods are unavailable. Therefore, we assumed a
244 5% infection prevalence among adults, consistent with the limited field data available (Lyons
245 1972; Steib & Mayer 1988; Garrett *et al.* 2020), corresponding with $\lambda = 0.0034$/day. Further,

246 while parasites are likely introduced in discrete pulses (a single mature female can introduce 1
247 million L1 larvae (Greenwood 2012)), we implemented a constant force of infection to avoid
248 confounding results with day of introduction. Lastly, we assumed infected adults cannot
249 reproduce (Moorthy 1938).

250 Using this model, we evaluated the consequences of episodic mortality events on stage-
251 specific and total abundance, with emphasis on the density of infectious copepods, the proximate
252 hazard to definitive hosts. We plotted the temporal dynamics for the 90% mortality scenario, a
253 previously used metric for Abate™ success (South Sudan Guinea Worm Eradication Program
254 2013). We plotted mean densities of all stages across the whole simulation period for scenarios
255 ranging from 0-90% mortality.

256

257 **Results**

258 ***Copepod population dynamics and mortality events***

259 Regardless of removal intensity, we found no significant decreases in mean population density
260 over the first 14-weeks of the study for size-unbiased (light blue) or size-biased (dark blue)
261 removal (Fig. 1). This apparent failure was consistent for both the total population and when
262 broken down by stage (Fig. 1, diamond, triangle, circle; all Dunnett's test $P > 0.05$).

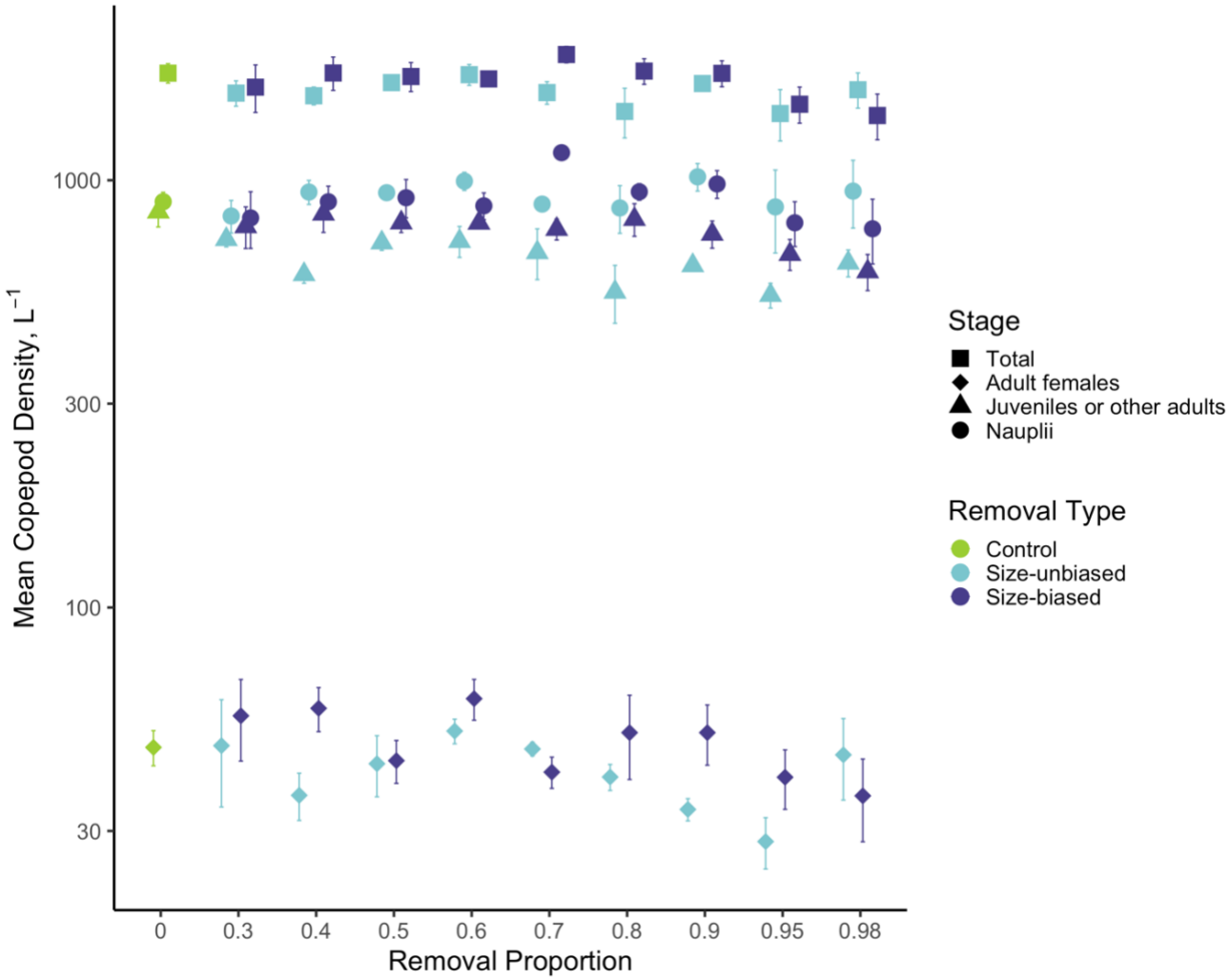

Figure 1. Mean observed copepod densities in the experiment over the 14 weeks in which the interventions were applied on schedule. Points and error bars represent treatment means ± SEs (log-transformed). Regardless of treatment type or removal proportion, there were no significant reductions in total copepod density (squares), or stage-specific densities of egg-bearing adult females (AF; diamonds), juveniles plus other adults (JOA; triangles), or nauplii (N; circles). Similar dynamics were observed regardless of whether removal was selective for large-bodied individuals (size-biased; dark blue) or equally applied across all stages (size-unbiased; light blue).

While we found no effect on mean density, the interventions did reduce densities immediately after application (e.g., 95 and 98% removal, Fig. 2, Supplemental S5). However, populations then rapidly rebounded. Populations in controls started at ~500-1,000 copepods/L, grew slowly for several weeks, and ended with a boom and bust (Fig. 2). In other cases, density in culled tanks temporarily surpassed controls, indicating overcompensation. For example, following the third intervention, densities in the 50% size-biased treatment were briefly higher than controls. In some cases, population recovery occurred so rapidly that declines were imperceptible one week later (e.g., after the second intervention with 80% removal). The best fit of the model generally captured the dynamics in intervention tanks better than that of the control treatment, which is partially expected, as the control treatment represented only 10% of the experiment.

Size-biased Removal:

Relative to controls, the 30% and 60% size-biased treatments grew steadily throughout the entire experiment (Fig. 2, Supplemental S5A). Populations quickly recovered from interventions, and observed dynamics generally fell within 95% credible intervals of the fitted model predictions. The 40%, 50%, and 70% removal treatments more closely resembled the controls, with large fluctuations in density at the end of the experiment. The 80%, 90%, and 95% removal treatments had multiple extreme booms and busts. Finally, 98% removal treatments fluctuated with low levels of population growth. These shifts sometimes fell outside the credible interval of posterior predictions.

Size-unbiased Removal:

In contrast with controls, 30%, 70% and 80% size-unbiased removal treatments maintained relatively constant abundances across all eighteen weeks, mostly within the credible

interval (Fig. 2, Supplemental S5A). The 40% and 60% tanks resembled the controls. The 50% treatment also resembled the control; however, instead of final booms and busts, populations declined steadily. The 90%, 95%, and 98% treatments had sustained peaks and troughs, encompassed by the credible interval for most of the experiment. The last few weeks had more extreme booms and busts, not captured within the credible interval.

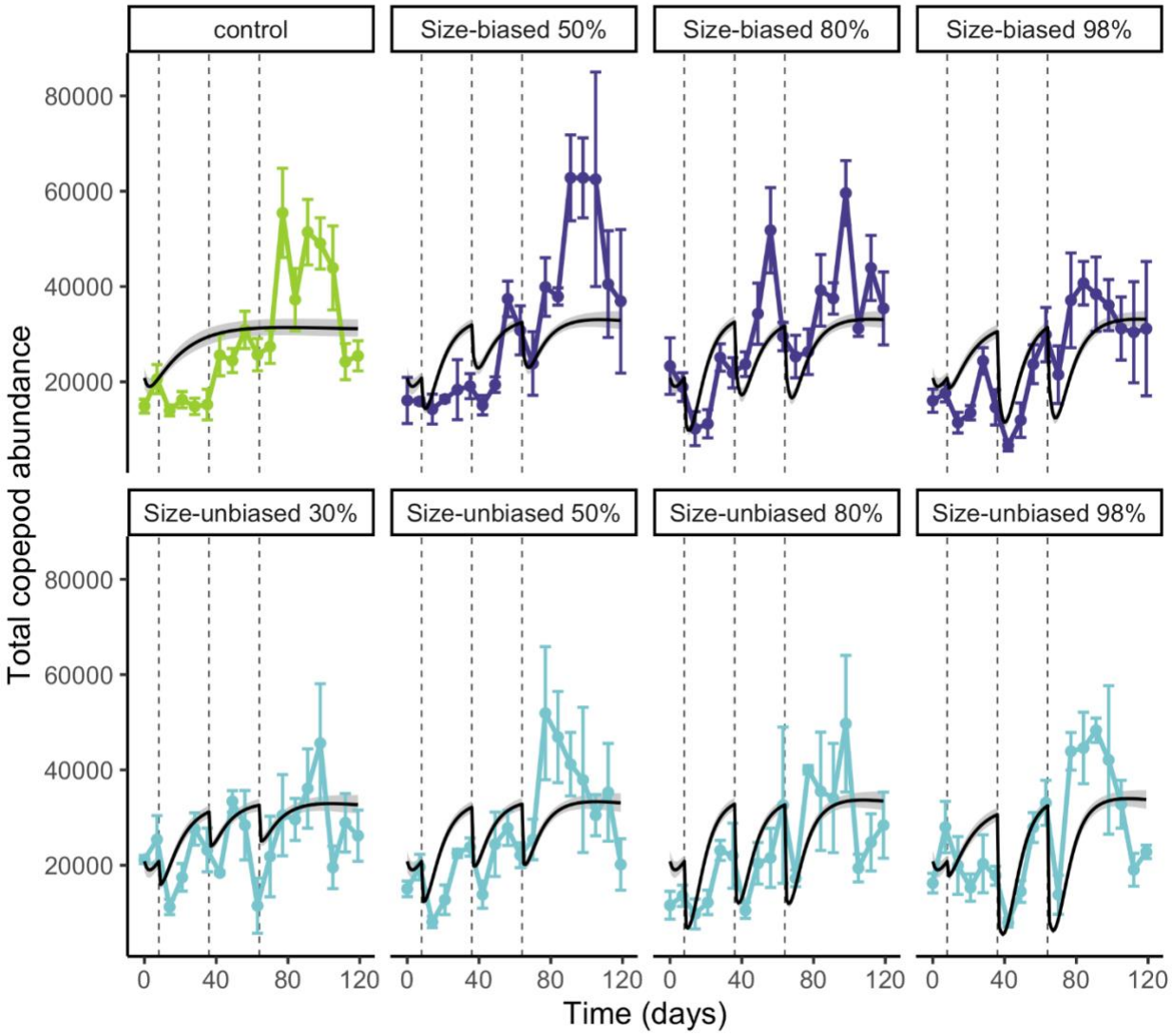

Figure 2. Observed copepod population dynamics (points and error bars represent means ± SE) and best-fitting posterior predictions with 95% credible intervals (black lines and shaded grey regions). Treatments that are representative of the major population dynamics are shown, with all

treatments can be found in the supplemental (Supplemental S5A). Dynamics in control tanks are plotted in green, size-biased removal tanks are plotted in light blue, and size-unbiased removal tanks are in dark blue. Dashed vertical lines represent interventions. In general, interventions caused immediate reductions in copepod abundance, but populations rebounded rapidly. In some case, e.g., size-biased 50% and size-unbiased 90%, these rebounds surpassed abundances observed in controls. For the 98% treatments, the first intervention was 20% removal, explaining the small dip in the model fit.

Evaluating the Functional Forms of Density Dependence

The strength of negative density dependence varied significantly across processes of birth, maturation, background death, and cannibalism. Density dependence was greatest for maturation rates, with a >18,000-fold reduction across the observed density gradient (Fig. 3). Density dependence on background death rate and cannibalism were also substantial, with a combined 4.4-fold increase over the density range (Fig. 3). However, we estimated essentially no effect on birth rates, with <2% decrease over the density range.

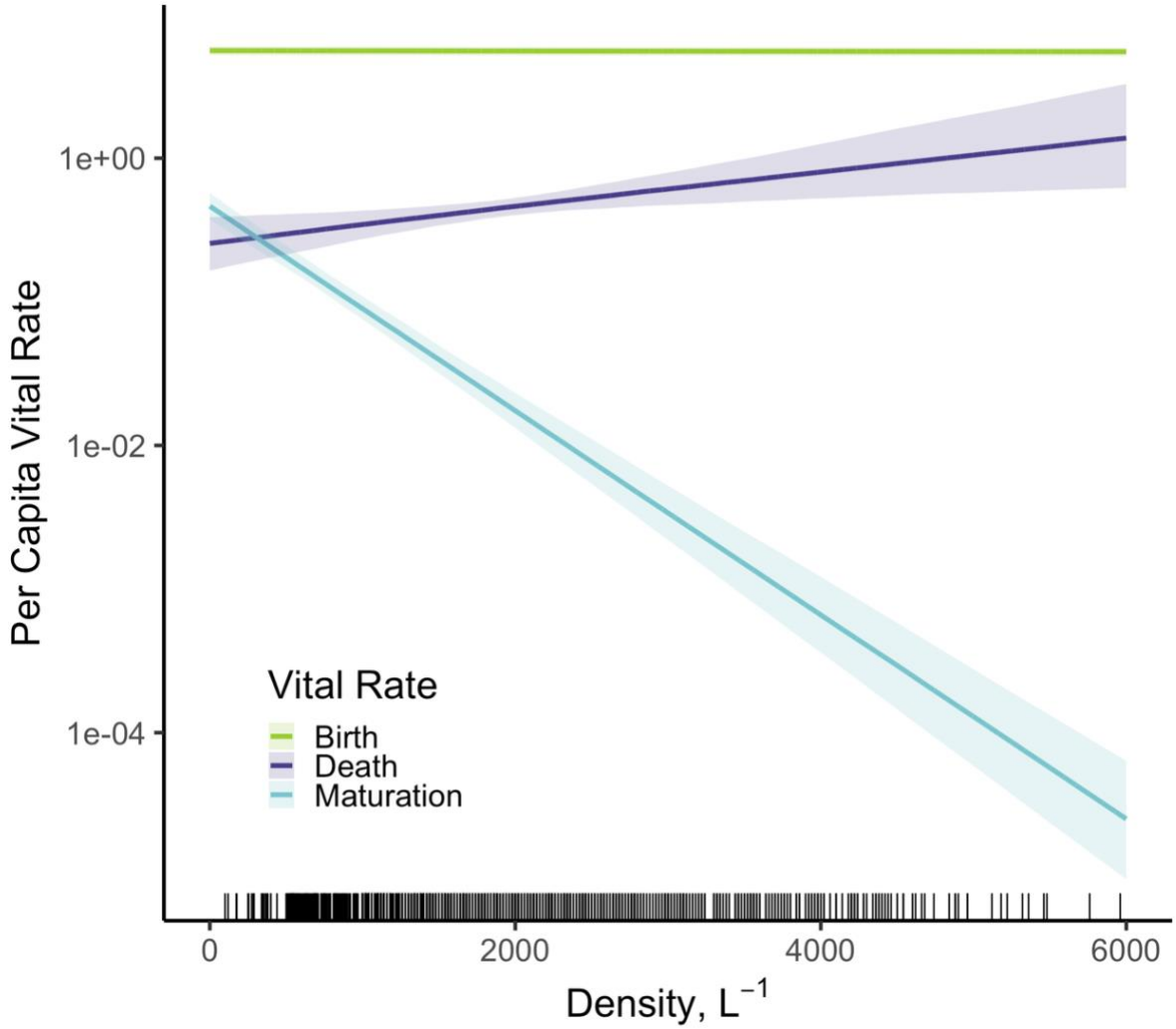

Figure 3. Representation of the sources of negative density dependence affecting copepod populations subject to control interventions. Lines and shaded regions represent mean and 95% credible intervals for posterior model predictions for the effects of copepod population density (with fixed stage structure) on key vital rates: birth rate (green), total death rate of nauplii (dark blue; incorporating background deaths and cannibalism via adults), and naupliar maturation rate (light blue). The rug indicates the observations of population density in the experiment. Adult birth rate was insensitive to competition, declining only 0.9% over the observed density gradient (indicated by the rug along the x-axis). In contrast, death rate increased 4.4-fold over the density

329 gradient. Most importantly, maturation rate was extremely sensitive, declining >18,000 fold over
330 the gradient.

331 ***Transmission Scenario Simulation Results***

332 Simulated GW infection scenarios exhibited rapid, stage-specific recovery of copepods
333 following interventions (Fig. 4). With 90% intervention intensity, nauplii and non-infectious
334 adults rapidly rebounded to densities that surpassed those observed for untreated populations
335 (Fig. 4C, D), and juveniles reached similar, though lower densities until the next intervention
336 (Fig. 4B). Size-unbiased removal generally reduced copepod populations more strongly, but
337 these populations also showed slightly greater overcompensation (Fig. 4A, C). This transient
338 overcompensation reiterated a central result from the experiment (Fig. 1): that mean copepod
339 density appeared unaffected by interventions.

340 Despite this apparent failure, simulated interventions successfully reduced the density of
341 infectious copepods (Fig. 4A). Without intervention, control populations began with low
342 densities of infectious hosts, but these grew steadily (>75 infected copepods L^{-1} by the end of the
343 100-day simulation). However, both size-unbiased and size-biased suppressed infectious
344 copepod density below 10 L^{-1} (Fig. 4A). Evaluating mean densities of stages across an
345 intervention intensity gradient (Fig. 5), total population density and non-infected adults
346 (susceptible + exposed classes) remained relatively constant at all intensities, while the density of
347 infectious adults steadily declined across the gradient. Thus, despite observing that copepod
348 populations rebound rapidly – enabled by intense density dependence on maturation rates – the
349 density of infectious hosts, the proximate source of mammalian infections, is highly sensitive to
350 intervention.

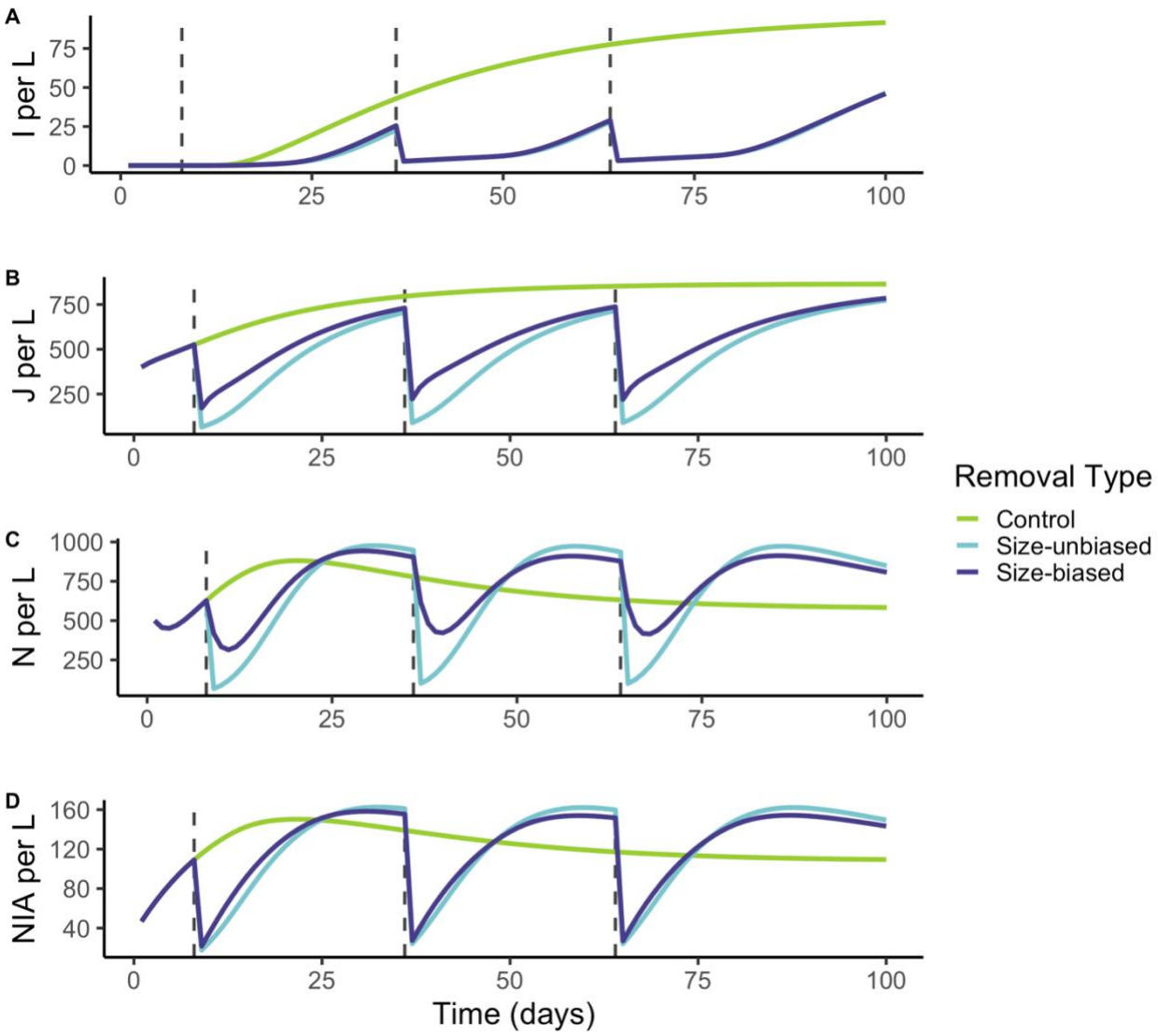

Figure 4. Temporal dynamics from the modeled transmission scenarios incorporating 90% mortality events at 28-day intervals. Dashed vertical lines represent interventions. Copepod stages are shown in different colors. Stages are divided into infectious adults (I), juveniles (J), nauplii (N), and non-infectious adults (NI = susceptible + exposed adults). Control tanks are dashed lines, 90% size-unbiased removal are solid lines, and 90% size-biased removal are the dotted lines. The force of infection parameter (λ =0.0034) corresponded with a ~5% infection rate among adults(Lyons 1972; Steib & Mayer 1988; Garrett *et al.* 2020). Nauplii and non-infected adults surpass densities of controls (green) with both forms of removal (size-biased

[dark blue] and size-unbiased [light blue]). Juveniles nearly recover to densities akin to controls. Most importantly, infectious copepods are severely depressed by both removal types.

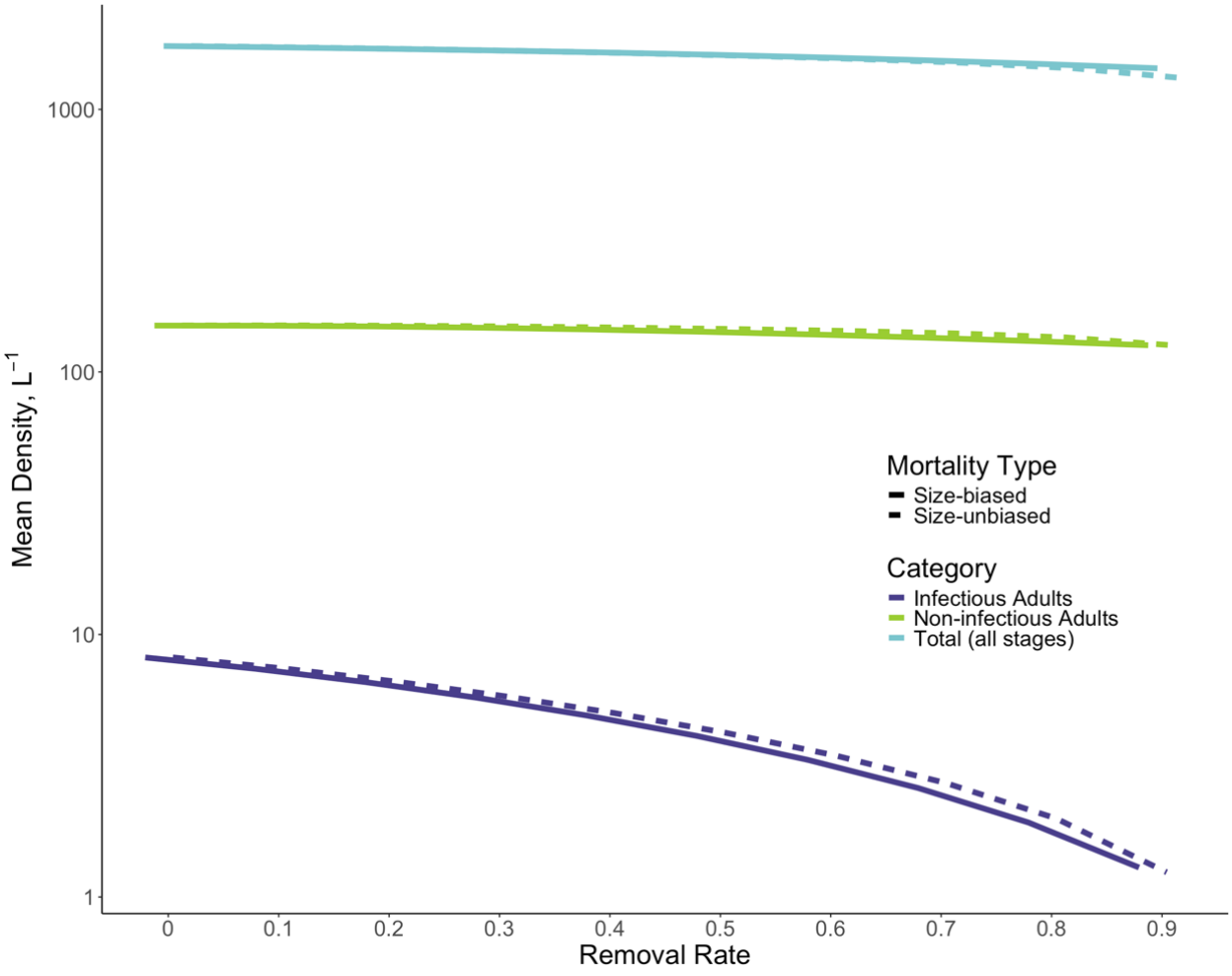

Figure 5: Mean total density of copepod populations (light blue), non-infectious adults (green), and infectious adults (dark blue) in 120-day transmission scenarios modeled along a gradient of intervention intensity for size-biased (solid line) and size-unbiased (dashed line) strategies. As in the experiment, total density and the density of non-infectious adults (susceptible and exposed) were largely insensitive to interventions, remaining relatively constant despite 90% population reductions imposed every 28 days. In contrast, the mean density of infectious adults, the proximate driver of mammalian hazard of infection, decreased almost 10-fold along the same

370 gradient. Thus, despite the rapid recovery of copepod populations and the appearance of failed
371 control, intervention can be highly effective at reducing the proximate driver of infection in
372 humans and other mammals.
373
374 **Discussion**
375 Uncovering the mechanisms regulating populations is a fundamental goal in population
376 ecology (Kaspersson *et al.* 2013; Karatayev *et al.* 2015). We combined a pest control experiment
377 and mechanistic modeling to partition the magnitude and importance of four general putative
378 mechanisms of density regulation. Then, we integrated these empirically-derived regulating
379 effects with a transmission model to evaluate how relaxation of density dependence via realistic
380 control methods shapes effectiveness of interventions for GW, a target for global parasite
381 eradication (Pellegrino *et al.* 2022).

382 Our experiment investigated how copepod populations – intermediate hosts of GWD –
383 responded to periodic culling. We designed treatments to mimic the treatment of water sources
384 with Abate™, an intervention commonly used to prevent GWD in endemic countries. We
385 hypothesized that more aggressive control efforts would better suppress copepod populations,
386 but that relaxed density dependence might lead to overcompensation. Strikingly, even when we
387 episodically removed up to 98% of the population, densities across were statistically
388 indistinguishable from controls (Fig. 1, Supplemental S3). Similar rebounds have been observed
389 in other copepod species, including *Mesocyclops leuckarti* which overshot pre-treatment
390 densities following application of Triphenyltin, a fungicide (Kulkarni *et al.* 2014). Our
391 interventions had failed to reduce copepod densities, an alarming prospect as other apparent pest
392 control failures have posed immense challenges for public health and conservation practitioners

393 (Rivero *et al.* 2010; Neale & Juliano 2019; Grosholz *et al.* 2021). For example, populations of
394 mosquitoes, sand flies, assassin bugs, and fleas, which are routinely treated to control diseases
395 such as malaria, leishmania, chagas, and plague, respectively, show evidence of insecticide
396 resistance, threatening vector control (Cao *et al.* 2025). Further, specific mosquito species
397 including *Aedes* and *Culex sp.*, vectors of diseases such as dengue, chikungunya, Zika virus
398 (*Aedes*) (Patterson *et al.* 2016), and West Nile Virus (*Culex*) (Hamer *et al.* 2008), show evidence
399 of culling-induced overcompensation, indicating that control strategies must be careful to not
400 impose mortality at levels that lead to overcompensatory releases from density dependence
401 (Neale & Juliano 2019). A striking example of a pest control program that backfired is the effort
402 to eliminate the invasive European green crab in an estuary off of California (Grosholz *et al.*
403 2021). Culling of green crabs was an effective strategy for years until the population density was
404 reduced below a critical threshold, triggering stage-specific overcompensation in recruitment
405 (Grosholz *et al.* 2021). The result was a boom in juvenile crabs, a shift in size structure, and
406 exacerbation of negative impacts (Grosholz *et al.* 2021). Together, these examples underscore
407 the challenges of pest control – especially in light of stage structure.

408 To attempt to further explain the surprisingly fast recovery we observed, we investigated
409 the forms of density dependence regulating *Eucyclops sp.* populations. Few studies have parsed
410 specific drivers of density dependence in natural populations. In one example, stocking large
411 brown trout reduced the growth rate of smaller individuals (Kaspersson *et al.* 2013). In another,
412 dynamics of Swedish vole populations were consistent with density dependence in recruitment
413 alone (Lambin *et al.* 2025). Stage-specific density dependence in maturation rates has been
414 documented in some ecological systems (Karatayev *et al.* 2015; Walker *et al.* 2021), including
415 other copepods (Kulkarni *et al.* 2014), allowing for population persistence under significant

416 mortality (Karatayev *et al.* 2015). We determined that density dependence in *Eucyclops sp.* was
417 driven predominantly by maturation rates, with a >18,000-fold reduction along the density
418 gradient, with a modest ~4.4-fold increase in total mortality, and no change in birth rate (Fig. 3).
419 Thus, when interventions occur, surviving adults maintain birth rates, but nauplii mature
420 extremely quickly. Consequently, higher proportions of nauplii and juveniles survive to
421 development, enabling rapid recovery and temporary overcompensation. (Figs. 2 and 4).

422 For the goal of GWD management, the failure to reduce mean copepod population
423 densities seems alarming. However, not all copepod life stages host GW, (McCullough 1983;
424 Bimi 2007) and there is a significant delay between copepod exposure to GW and infectiousness
425 to mammals (~15 days; Gonzalez Engelhard *et al.* 2021). Thus, we speculated that if population
426 rebounds were driven by overcompensation in young stages that cannot transmit GW, then
427 apparent failures to control the overall population might actually conceal successes. We
428 evaluated this possibility by extending our model to include GW infection of adults with a
429 distributed delay from the exposed to infectious class. We tracked changes in the density and
430 stage structure of copepod populations across a gradient of intervention intensity.

431 When we simulated GW transmission scenarios, we found strong support for stage-
432 specific recovery dynamics, as documented in other zooplankton systems (Nilsson *et al.* 2010;
433 Kulkarni *et al.* 2014). Specifically, the densities of nauplii, juveniles, and non-infectious adults
434 all recovered rapidly to meet or exceed pre-intervention densities following each successive
435 mortality event (Fig. 4), indicating compensation or overcompensation (Abrams 2009; Kulkarni
436 *et al.* 2014; de Roos 2020; Grosholz *et al.* 2021). Critical to GW transmission, the density of
437 infectious adults remained extremely low. Thus, despite the apparent failure of these
438 interventions to control copepod populations, they appear highly effective at specifically

439 controlling the life stage that is the proximate cause of GW infections. We attribute this effect to
440 the approximately15-day developmental period from first stage to infectious third stage GW
441 larvae (Lindquist & Cross 2017; Gonzalez Engelhard *et al.* 2021), which is long enough to
442 prevent accumulation of infectious copepods before each successive intervention (Fig 4., Fig. 5).
443 Similar lags of parasite development in intermediate hosts and vectors are present in other
444 systems. For example, in Anopheline mosquitoes, a 2-3 week incubation period separates vector
445 exposure to *Plasmodium* and infectiousness to humans (Crutcher JM 1996). Similarly,
446 *Trypanosoma* maturation in tsetse flies requires approximately three weeks (Telleria *et al.* 2014).
447 Thus, reducing the overall density of intermediate hosts or vectors may not be essential for
448 success if control can cause high turnover in the stage(s) responsible for transmission.

449 Our results raise the importance of field surveillance targeted at infected copepods. At
450 present, diagnosing infections in copepods from field is infeasible due to GW rarity and the scale
451 of geographic surveillance (Pellegrino *et al.* 2022). Therefore, current eradication programs rely
452 on monitoring the total density of copepods before and after Abate™ applications. If copepod
453 communities in the field recover as rapidly as the *Eucyclops sp.* examined in our study, officials
454 might falsely conclude that control is ineffective, because population densities return to pre-
455 treatment levels every month. However, our experiment and model suggest that this observation
456 could conceal a cryptic success: reduction in the density of infectious copepods. Thus, we
457 recommend the development of tools to facilitate large-scale spatial and temporal diagnostics of
458 GW-infected copepods to evaluate the relevance of this counterintuitive finding.

459 We note some important caveats to translating these insights to the field. First, we
460 focused on a single copepod isolate. Greater understanding of copepod diversity in demographic
461 rates and sensitivity to Abate™ would greatly benefit eradication programs. Second, we

implemented mechanical removal, which enabled a precise experimental design, but can differ from chemical control. Experiments with Abate™ are needed to evaluate chemical persistence, delayed or sublethal effects, and the consequences of over- or underdosing. Lastly, our analysis identified high importance for negative density dependence on maturation rates and mortality, and no effect on birth rates. Generally, the model fit the data well for the first 70-80 days of the experiment, albeit with some initial lags in population growth (Fig. 2). This imperfect fit could be due to missing key processes in the model, such as an Allee effect, where mating failure occurs at low population densities (seen for copepods (Kramer *et al.* 2008)). The inability of the model to precisely recover empirical dynamics could also be due to nonconstant conditions in the tanks (e.g., the accumulation of nutrients (Sahandi *et al.* 2023) and/or waste products or differences in temperature or photoperiod over the course of the experiment). Nevertheless, the POMP approach has major benefits, including representation of constraints in the observation process and incorporation of process noise. Lastly, future studies of copepod control and recovery could consider other functional forms for key demographic processes, including Type-II or Type-III functional responses for cannibalism.

Chemical control of copepod populations represents a critical intervention for national GW eradication programs (Gindola *et al.* 2022). This study highlights that nuance may be needed to evaluate this intervention: population dynamics may suggest that control efforts are failing or even backfiring, but direct analyses of infectious copepods, the proximate cause of human cases and animal infections should be prioritized. Future laboratory studies should expand to greater copepod diversity and directly evaluate pesticide formulations in use. Ultimately, a deeper understanding of copepod control may improve the portfolio of GWD interventions and contribute to the eradication of this devastating parasite.

More broadly, pest control is inherently designed to reduce population density (Ni *et al.* 2025), so understanding density dependence is critical to predicting responses (McIntire & Juliano 2018). This work underscores the value of defining which life stages of pests are most impactful, elucidating how stage-structured pest populations respond to interventions, and developing a mechanistic understanding of density dependent mechanisms regulating populations under control, especially in cases where focal populations experience drastic and rapid shifts in density. Together, this information can be applied to anticipate and explain potentially counterintuitive consequences of interventions. A thorough understanding of these dynamics is critical for forecasting long-term population trajectories and their sensitivity to density-dependent perturbations, paramount to predicting the influence of environmental and ecological stressors on population dynamics.

Acknowledgements

This work was supported by funding from The Carter Center. We thank the Programme National d'Eradication du Ver de Guinée - Tchad for collecting and providing the Chadian *Eucyclops sp.* copepods used in our study, and the Yen lab at the Georgia Institute of Technology for providing the culture to us. We thank The Carter Center and other Civitello lab members for feedback on this manuscript. We also thank M. Hoogshagen and J. Raytselis for helping with sampling over the holidays, and B. Lukubye for moral support.

Literature Cited

1.

Abrams, P.A. (2009). When does greater mortality increase population size? The long history and diverse mechanisms underlying the hydra effect. *Ecology Letters*, 12, 462-474.

2.

Bimi, L. (2007). Potential vector species of Guinea worm (Dracunculus medinensis) in Northern Ghana. *Vector Borne Zoonotic Dis*, 7, 324-329.

3.

Bolker, B. (2017). {glmmTMB} Balances Speed and Flexibility Among Packages for Zero-inflated Generalized Linear Mixed Modeling.

4.

Calizza, E., Costantini, M.L., Careddu, G. & Rossi, L. (2017). Effect of habitat degradation on competition, carrying capacity, and species assemblage stability. *Ecology and Evolution*, 7, 5784-5796.

5.

Cao, L.J., Chen, J.C., Thia, J.A., Schmidt, T.L., Ffrench-Constant, R., Zhang, L.X. *et al.* (2025). Recurrent mutations drive the rapid evolution of pesticide resistance in the two-spotted spider mite Tetranychus urticae. *Elife*, 14.

6.

Carles Bretó, J.W., Aaron A. King, and Edward L. Ionides (2025). panelPomp: Analysis of Panel Data via Partially Observed Markov Processes in R. *The R Journal*.

7.

Choi, L., Majambere, S. & Wilson, A.L. (2019). Larviciding to prevent malaria transmission. *Cochrane Database Syst Rev*, 8, Cd012736.

8.

Crutcher JM, H.S. (1996). *Malaria*, Medical Microbiology.

9.

de Roos, A. (2020). The impact of population structure on population and community dynamics. pp. 53-73.

10.

Dennis, B., Desharnais, R.A., Cushing, J.M., Henson, S.M. & Costantino, R.F. (2001). Estimating Chaos and Complex Dynamics in Insect Populations *Ecological Monographs*, 71, 277-303.

11.

Endo, A., van Leeuwen, E. & Baguelin, M. (2019). Introduction to particle Markov-chain Monte Carlo for disease dynamics modellers. *Epidemics*, 29, 100363.

12.

Garrett, K.B., Box, E.K., Cleveland, C.A., Majewska, A.A. & Yabsley, M.J. (2020). Dogs and the classic route of Guinea Worm transmission: an evaluation of copepod ingestion. *Sci Rep*, 10, 1430.

13.

Gindola, Y., Getahun, D., Mohammed, K., Kamau, E., Camara, B., Wossen, M. *et al.* (2022). Abate application practices in the Guinea worm endemic region of Gambella, Ethiopia: identification of elimination gaps. *The Journal of Infection in Developing Countries*, 16, 20S-25S.

14.

Gonzalez Engelhard, C.A., Hodgkins, A.P., Pearl, E.E., Spears, P.K., Rychtář, J. & Taylor, D. (2021). A mathematical model of Guinea worm disease in Chad with fish as intermediate transport hosts. *Journal of Theoretical Biology*, 521, 110683.

15.

Gotelli, N. (2008). *A Primer of Ecology* Fourth edn.

16.

Greenwood, D. (2012). 63 - Helminths: Intestinal worm infections; filariasis; schistosomiasis; hydatid disease. In: *Medical Microbiology (Eighteenth Edition)* (eds. Greenwood, D, Barer, M, Slack, R & Irving, W). Churchill Livingstone Edinburgh, pp. 655-666.

17.

Grosholz, E., Ashton, G., Bradley, M., Brown, C., Ceballos-Osuna, L., Chang, A. *et al.* (2021). Stage-specific overcompensation, the hydra effect, and the failure to eradicate an invasive predator. *Proceedings of the National Academy of Sciences*, 118, e2003955118.

18.

Grunert, R., Box, E., Garrett, K., Yabsley, M. & Cleveland, C. (2022). Effects of Temephos (Abate®), Spinosad (Natular®), and Diflubenzuron on the Survival of Cyclopoid Copepods. *Am J Trop Med Hyg*, 106, 818-822.

19.

Hamer, G.L., Kitron, U.D., Brawn, J.D., Loss, S.R., Ruiz, M.O., Goldberg, T.L. *et al.* (2008). Culex pipiens (Diptera: Culicidae): A Bridge Vector of West Nile Virus to Humans. *Journal of Medical Entomology*, 45, 125-128.

20.

Hanazato, T., Iwakuma, T., Yasuno, M. & Sakamoto, M. (1989). Effects of temephos on zooplankton communities in enclosures in a shallow eutrophic lake. *Environmental Pollution*, 59, 305-314.

21.

Hixon, M.A. & Jones, G.P. (2005). Competition, Predation, and Density-Dependent Mortality in Demersal Marine Fishes *Ecology*, 86, 2847-2859.

22.

Hurtado, P.J. & Kirosingh, A.S. (2019). Generalizations of the 'Linear Chain Trick': incorporating more flexible dwell time distributions into mean field ODE models. *J Math Biol*, 79, 1831-1883.

23.

Johnson, S.N. & Rasmann, S. (2015). Root-feeding insects and their interactions with organisms in the rhizosphere. *Annu Rev Entomol*, 60, 517-535.
24.

Karatayev, V.A., Kraft, C.E. & Zipkin, E.F. (2015). Racing through life: maturation rate plasticity regulates overcompensation and increases persistence. *Ecosphere*, 6, art203.
25.

Kaspersson, R., Sundström, F., Bohlin, T. & Johnsson, J.I. (2013). Modes of Competition: Adding and Removing Brown Trout in the Wild to Understand the Mechanisms of Density-Dependence. *PLOS ONE*, 8, e62517.
26.

Kilham, S., Kreeger, D., Lynn, S., Goulden, C. & Herrera, L. (1998). COMBO: A defined freshwater culture medium for algae and zooplankton. *Hydrobiologia*, 377, 147-159.
27.

Kramer, A.M., Sarnelle, O. & Knapp, R.A. (2008). Allee Effect Limits Colonization Success of Sexually Reproducting Zooplankton. *Ecology*, 89, 2760-2769.
28.

Kulkarni, D., Hommen, U., Schäffer, A. & Preuss, T.G. (2014). Ecological interactions affecting population-level responses to chemical stress in Mesocyclops leuckarti. *Chemosphere*, 112, 340-347.
29.

Lambin, X., Begon, M., Burthe, S.J., Graham, I.M., MacKinnon, J.L., Telfer, S. *et al.* (2025). Density-dependent recruitment but not survival drives cyclic dynamics in a field vole population. *Proceedings of the National Academy of Sciences*, 122, e2509516122.
30.

Leboulanger, C., Schwartz, C., Somville, P., Diallo, A.O. & Pagano, M. (2011). Sensitivity of Two Mesocyclops (Crustacea, Copepoda, Cyclopidae), from Tropical and Temperate Origins, to the Herbicides, Diuron and Paraquat, and the Insecticides, Temephos and Fenitrothion. *Bulletin of Environmental Contamination and Toxicology*, 87, 487-493.
31.

Lenth, R.V. (2025). emmeans: Estimated Marginal Means, aka Least-Squares Means.
32.

Lindquist, H.D.A. & Cross, J.H. (2017). 195 - Helminths. In: *Infectious Diseases (Fourth Edition)* (eds. Cohen, J, Powderly, WG & Opal, SM). Elsevier, pp. 1763-1779.e1761.
33.

Lu, A. & Wang, L. (2025). Hygiene conditions explain larval density-dependent performance in Plutella xylostella with sufficient food. *Journal of Asia-Pacific Entomology*, 28, 102444.
34.

Lyons, G.R. (1972). Guineaworm infection in the Wa district of north-western Ghana. *Bull World Health Organ*, 47, 601-610.

35.

McCullough, F.S. (1983). Cyclopoid copepods: their role in the transmission and control of dracunculiasis. (ed. Press, NA). World Health Organization, Geneva Ecology and Control of Vectors Unit, Division of Vector Biology and Control.
36.

McIntire, K.M. & Juliano, S.A. (2018). How can mortality increase population size? A test of two mechanistic hypotheses. *Ecology*, 99, 1660-1670.
37.

Moorthy, V.N. (1938). Observations on the development of Dracunculus medinensis larvae in Cyclops. *American Journal of Hygiene*.
38.

Neale, Z.R. & Juliano, S.A. (2019). Finding the sweet spot: What levels of larval mortality lead to compensation or overcompensation in adult production? *Ecosphere*, 10, e02855.
39.

Newman, K., King, R., Elvira, V., de Valpine, P., McCrea, Rachel S. & Morgan, B.J.T. (2023). State-space models for ecological time-series data: Practical model-fitting. *Methods in Ecology and Evolution*, 14, 26-42.
40.

Ni, J., Wang, J., Zhang, W., Chen, E., Gao, Y., Sun, J. *et al.* (2025). Sustainable control and integrated management through a one health approach to mitigate vector-borne disease. *One Health*, 20, 101018.
41.

Nilsson, K.A., Persson, L. & Van Kooten, T. (2010). Complete compensation in Daphnia fecundity and stage-specific biomass in response to size-independent mortality. *Journal of Animal Ecology*, 79, 871-878.
42.

Park, T., Mertz, D.B., Grodzinski, W. & Prus, T. (1965). Cannibalistic Predation in Populations of Flour Beetles. *Physiological Zoology*, 38, 289-321.
43.

Patterson, J., Sammon, M. & Garg, M. (2016). Dengue, Zika and Chikungunya: Emerging Arboviruses in the New World. *West J Emerg Med*, 17, 671-679.
44.

Pellegrino, C., Patti, G., Camporeale, M., Belati, A., Novara, R., Papagni, R. *et al.* (2022). Guinea Worm Disease: A Neglected Diseases on the Verge of Eradication. *Trop Med Infect Dis*, 7.
45.

R Core Team (2023). R: A Language and Environment for Statistical Computing.
46.

Rivero, A., Vézilier, J., Weill, M., Read, A.F. & Gandon, S. (2010). Insecticide Control of Vector-Borne Diseases: When Is Insecticide Resistance a Problem? *PLOS Pathogens*, 6, e1001000.

47.

Sahandi, J., Sorgeloos, P., Xiao, H., Mu, F., Wang, X., Qi, Z. *et al.* (2023). The use of microbes in culture of harpacticoid copepod (Tigriopus japonicus Mori) for suppression of Vibrio and enhancement of population growth, enzyme activity and microbial longevity. *Aquaculture*, 563, 739008.

48.

Sebens, K.P. (1982). Competition for Space: Growth Rate, Reproductive Output, and Escape in Size. *The American Naturalist*, 120, 189-197.

49.

Simonetti, O., Zerbato, V., Maurel, C., Cosimi, L., Babich, S., Cavalli, F. *et al.* (2023). The current state of knowledge on dracunculiasis: a narrative review of a rare neglected disease. *Infez Med*, 31, 500-508.

50.

Smith, G.C. (1997). An analysis of the form of density dependence in a simulation model of a seasonal breeder undergoing control. *Ecological Modelling*, 95, 181-189.

51.

South Sudan Guinea Worm Eradication Program (2013). Management and Technical Guidelines. (ed. Sudan, MoH-RoS).

52.

Steib, K. & Mayer, P. (1988). Epidemiology and vectors of Dracunculus medinensis in northwest Burkina Faso, West Africa. *Annals of Tropical Medicine & Parasitology*, 82, 189-199.

53.

Stockseth, L., Neale, Z. & Rudolf, V.H.W. (2025). Strengthening of negative density dependence mediates population decline at high temperatures. *Ecology*, 106, e70030.

54.

Svanbäck, R. & Bolnick, D.I. (2007). Intraspecific competition drives increased resource use diversity within a natural population. *Proceedings of the Royal Society B: Biological Sciences*, 274, 839-844.

55.

Telleria, E.L., Benoit, J.B., Zhao, X., Savage, A.F., Regmi, S., e Silva, T.L.A. *et al.* (2014). Insights into the Trypanosome-Host Interactions Revealed through Transcriptomic Analysis of Parasitized Tsetse Fly Salivary Glands. *PLOS Neglected Tropical Diseases*, 8, e2649.

56.

van den Bosch, F. & Gabriel, W. (1994). A model of growth and development in copepods. *Limnology and Oceanography*, 39, 1528-1542.

57.

704 van den Bosch, F. & Santer, B. (1993). Cannibalism in Cyclops abyssorum. *Oikos*, 67, 19-28.
705 58.

706 Walker, M., Robert, M.A. & Childs, L.M. (2021). The importance of density dependence in
707 juvenile mosquito development and survival: A model-based investigation. *Ecological*
708 *Modelling*, 440, 109357.
709 59.

710 World Health Organization (1986). Decisions and list of resolutions. World Health Assembly.
711 60.

712 World Health Organization (2025). Dracunculiasis (Guinea-worm disease).

713